Evaluating Nine Machine Learning Algorithms for GaN HEMT Small Signal Behavioral Modeling through K-fold Cross-Validation

Neda Ahmad
University School of Information, Communication and Technology, Guru Gobind Singh Indraprastha University, New Delhi, India
neda.21116490021@ipu.ac.in (corresponding author)

Vandana Nath
University School of Information, Communication and Technology, Guru Gobind Singh Indraprastha University, New Delhi, India
vandana.nath@ipu.ac.in

Received: 3 May 2024 | Revised: 26 May 2024 | Accepted: 3 June 2024

 DOI: https://doi.org/10.48084/etasr.7726

ABSTRACT

This paper presents an investigation into the modeling of Gallium Nitride (GaN) High Electron Mobility Transistors (HEMTs) using multiple Machine Learning (ML) algorithms. Despite the documented use of various ML techniques, a thorough comparison and performance analysis under different operating conditions were lacking. This study fills this gap by conducting a rigorous evaluation of nine ML models using TCAD-generated data of Pseudomorphic AlGaN/InGaN/GaN HEMT. The research focuses on Small Signal Behavioral Modeling and examines regression techniques such as Multiple Linear Regression (MLR), Multivariate Linear Regression (MVLR), Ridge Regression (L2), Lasso Regression (L1), Elastic Net Regression (ENR), Decision Trees (DT), Random Forest (RF), Gradient Boosting Regression(GBR), and Support Vector Regression (SVR). These methods use biases, frequency, and device geometry as independent variables, with S-parameters being the dependent variables. K-fold cross-validation was employed to ensure model reliability and accuracy across diverse operating conditions. Results reveal that the RF, coupled with 10-fold cross-validation, exhibits superior performance giving 99.7% accurate results, with a Mean Squared Error (MSE) of 4.6375×10^{-5}, and a coefficient of determination (R^2) of 0.9977. Conversely, SVR, L1, and ENR fall short of expectations. This study underscores the significance of methodological advancements in ML-based GaN HEMT modeling and provides valuable insights for future research in this domain.

Keywords-S-parameters; machine learning; HEMT; neural networks; modeling; regression

I. INTRODUCTION

Development of High Electron Mobility Transistors (HEMT) is a continuously growing research field. It is a transistor based on the principle of heterojunction typically composed of materials such as GaN/AlGaN forming a 2D electron gas channel, allowing for high-speed switching and amplification of signals [1, 2]. HEMTs have various advantages including low noise characteristics, high-frequency application, and high-power handling capacities which find applications in RF amplifiers, wireless communication systems, radar systems, microwave circuits, power amplifiers, power electronics, and high-power switching applications. The advent of gallium nitride (GaN) HEMTs can offer superior performance in terms of high power and high frequency compared to mainstream silicon and other advanced semiconductor Field-Effect Transistor (FET) technologies. This potential has been extensively reviewed in [3-5].

Small signal modeling in HEMT is crucial for accurately predicting the behavior of these semiconductor devices under varying input conditions, which is important for optimizing circuit design and performance. At high frequencies, voltage and current measurements are unsuitable for circuit analysis as they resemble traveling waves, which are measured by the S-parameters. Traditional methods often rely on complex mathematical equations derived from semiconductor physics, which can be computationally intensive and may not capture all nuances of device behavior [6-9]. Finding the optimal balance between accuracy and complexity is essential, as a greater number of circuit elements results in increased accuracy in the cost of increased complexity [10, 11]. An alternative approach to small signal modeling in HEMT is Machine Learning (ML) regression techniques. By training models on datasets containing input-output pairs, ML algorithms can learn complex patterns and relationships between input signals and device responses. Different regression techniques, such as

ANN, SVR, MLP etc. have been applied to predict small signal characteristics of HEMTs. When using typical learning prediction models, data sets are split into training, validation, and testing subsets. However, this approach has some disadvantages such as:

- **Data Leakage**: The set data can influence the model during training, making performance improvements seem insignificant.
- **Reduced Sample Size**: Splitting data into three sets reduces the number of samples available for learning and testing, potentially harming model performance.

To address these issues, Cross-Validation (CV) is used. CV helps prevent methodological errors by ensuring that the model does not see any unseen data until the final evaluation

In this paper, we explored nine different ML based models namely Multiple Linear Regression (MLR), Multivariate Linear Regression (MVLR), Ridge Regression (L2), Lasso Regression (L1), Elastic Net Regression (ENR), Decision Trees (DT), Random Forest (RF), Gradient Boosting Regression(GBR), and Support Vector Regression (SVR). These algorithms are compared and evaluated using K-fold CV instead of a single training-testing split. This method divides the dataset into K subsets (folds) and trains the model K times, each time using a different fold as the testing set and the remaining folds as the training set. This approach reduces the risk of overfitting and gives a more accurate estimate of the model's performance on unseen data. We evaluated all models using four different K values (3, 5, 7, 10) to compare the performance of various regression algorithms in predicting small signal characteristics of HEMTs. Additionally, we assessed how cross-validation strategies affect the generalizability and robustness of the models across different regression techniques and operating conditions.

II. LITERATURE REVIEW

Previous research [6-9, 12, 13] has primarily utilized conventional methods of extracting small signal models, failing to consider the potential of ML regression techniques. Table I shows the progress in employing ML techniques for HEMT modeling. The majority is based on only a few ML techniques which conclude that the ML application in HEMT modeling is still underexplored.

III. DATA SET AND METHODOLOGY

TCAD allows us to perform virtual experiments and simulations before fabricating the device, reducing development time and costs. As shown in Figure 1, the device built on the simulator has the following parameters: The substrate has a 400 µm SiC layer, graded AlN nucleation, and a 1.5 nm layer to minimize threading dislocations between the SiC substrate and 1.5 µm GaN buffer layer. A 5 nm GaN cap layer prevents Al oxidation and facilitates ohmic contacts after the 20 nm AlGaN supply layer. There is an undoped AlGaN spacer layer (25.3% Al) of 5 nm, then a 5 nm In0.10Ga0.90N layer between the GaN buffer and spacer.

TABLE I. PREVIOUS MODELS

Ref.	ML methods	Evaluation metrics	Remarks
2015 [14]	ANN	Accuracy	Noise parameter modeling
2018 [15]	ANN, SVM, DT	MSE	Modeling of I-V characteristics
2014 [16]	ANN	MAG and MSG	Temperature-dependent S-parameter modeling
2019 [17]	ANN-GA, PSO, GWO	Error rate	Combines ANN with various optimization techniques
2023 [18]	ANN	Execution time	Testing ANN on MATLAB, Python, and R software environments
2019 [19]	ANN	Percentage error	S-parameter modeling over several types of FET
2021 [20]	SVR	Accuracy	S-parameter error correction model
2020 [21]	SVR	Accuracy, percentage error	S-parameter modeling
2020 [22]	GA	MSE	Accuracy, S-parameter modeling
2021 [23]	ANN, SVR, PSO	MSE	S-parameter modeling
2020 [24]	ANN, GA, PSO, SVR, GPR	MSE	Large signal modeling
2017 [25]	GA, PSO, ABC	Percentage error	Parameter extraction and extrinsic parameter tuning and S-parameter simulation
2019 [26]	ANN-GA	Graphically measured value	Electrothermal modeling
2018 [27]	SVR	Graphically measured value	S-parameter modeling
2019 [28]	ANN, SVR, DT	MSE	S-parameter modeling
2019 [29]	NARX	MSE	S-parameter modeling
2019 [30]	Analytical and SVR	MSE, corelation coefficient	Parameter extraction and S-parameter modeling
2020 [31]	MLP and cascade structure	Accuracy, convergence rate, and generalization capability	Small signal modeling
2020 [32]	PSO, SVR	Accuracy	Small signal behavioral modeling
2021 [33]	GPR	MSE	Small signal modeling
2021 [34]	Distinct ANN architectures	MSE, MAE, fitting curves, and R^2	Small signal behavioral modeling
2022 [35]	RF	MAE, MSE	A cross-platform application predicts GaN high electron mobility device scattering (S-) parameter, gain, power, device width, and traps.
2022 [36]	SVR,GPR, DT, GA, ANN, RANdom SAmple Consensus,	MSE, MAE, R2	S-parameter small signal modeling
2023 [37]	MPA, POA, TSA	Execution time	Small signal parameter extraction and optimization

The dataset is generated considering various operating conditions, and the corresponding responses for different bias conditions are recorded as the S-parameters, concerning real and imaginary values (S11, S12, S21, S22). The measurement data are from the AlGaN/InGaN/GaN HEMT device. Step size

of 1 V is used to vary the gate-to-source voltage (V_{GS}) for both devices from –4 V to 2 V. In addition, the drain-to-source voltage (V_{DS}) is swept with a 2 V increment from 0 V to 16 V. The frequency (f) range of the device is 1 to 50 GHz, with a step size of 1 GHz and gate width Wg of 200 and 100 um. Combining the samples for each device generates the complete dataset used in this paper. The combined dataset comprises over 4000 samples and includes four predictor variables: V_{DS}, V_{GS}, f, and Wg. Furthermore, eight predicted variables are shown to exist: Real (Re) S11, imaginary (Imag) S11, Re S21, Imag S21, Re S12, Imag S12, Re S22, and imag S22. Figure 2 shows the proposed model structure. In the ML-based model 9 models along with K(3,5,7,10)-fold CV are compiled and analyzed.

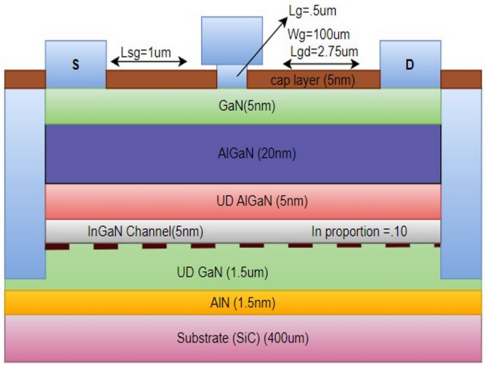

Fig. 1. Structure of the chosen AlGaN/InGaN/GaN HEMT.

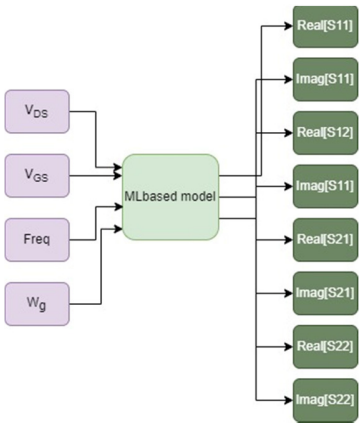

Fig. 2. Fig. 2. Structure of proposed model.

A. Data Preprocessing

Understanding the distribution of the dataset is crucial, as depicted in Figure 3, which illustrates the Re and Imag distribution of each S-parameter within the full dataset. Variability is observed among most parameters, with some exhibiting discontinuous output values that deviate from the overall distribution. Additionally, anomalies such as outliers and uneven peak values are apparent, likely stemming from measurement discrepancies. The disparity in ranges between predictors and predicted variables poses a significant challenge, distorting the error function's contour and leading to erroneous results, particularly in the algorithm's struggle to identify global minima, often converging at local minima. Moreover, outliers directly impact decision boundary placement, resulting in higher errors on testing sets. Outliers in datasets cause algorithms to react differently. For example, mean squared error function is more affected than mean absolute error function. Hence, it is imperative to address outliers and smooth peak values during preprocessing to ensure accurate analysis.

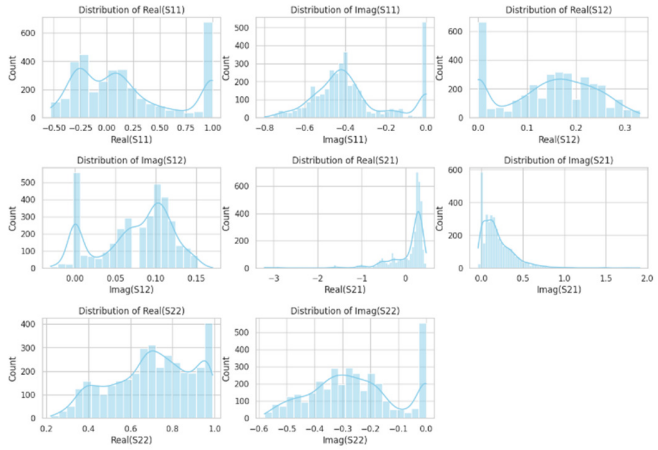

Fig. 3. Distribution of all 8 dependent variables.

B. Methodology

The flowchart exhibited in Figure 4 analyzes the methodology employed in this research paper, which has been thoroughly explained in the previous sections. Different models based on nine ML algorithms, namely MLR, MLVR, L2, L1, ENR, DT, RF, GBR, SVR, are compared and evaluated [38].

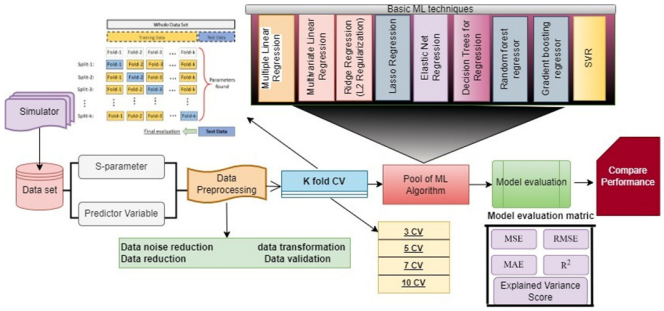

Fig. 4. Flow diagram of the proposed methodology.

TABLE II. ERROR MATRIC USED FOR MODEL EVALUATION[39]

Error	Equation
Mean Absolute Error (MAE)	$\frac{1}{n}\sum_{i=1}^{n}\left\|y_i-\hat{y}_i\right\|$
Mean Squared Error (MSE)	$\frac{1}{n}\sum_{i=1}^{n}\left(y_i-\hat{y}_i\right)^2$
Root Mean Squared Error (RMSE)	$RMSE=\sqrt{MSE}$
R-squared (R^2)	$1-\frac{\sum_{i-1}^{n}(y_i-\hat{y}_i)^2}{\sum_{i-1}^{n}(y_i-y)^2}$
Explained Variance Score	$1-\frac{\mathrm{Var}(y-\hat{y})}{\mathrm{Var}(y)}$

IV. RESULT AND DISCUSSION

An exhaustive analysis and comparison of nine ML based algorithms, namely MLR, MLVR, L2, L1, ENR, DT, RF, GBR, and SVR were evaluated using different K(3,5,7,10)-fold cross-validation techniques. The performance of each algorithm was assessed using MSE, MAE, R2, RMSE, and EVS. Figures 5-9 manifest a comparison bar graph of all the models with all the four k-fold validation clubbed for each error parameter. Figure 5 presents the least MAE for DT, RF, and GBR, whereas Lasso and SVR show higher value. MLR exhibits the worst MAE comparatively. The MSE graph in Figure 6 exhibits a trend similar to MAE, making MLR worse and DT, RF, and GBR comparably having the best results. In Figure 7, the RMSE graph presents the RF regression as the best model, MLR as unfit, and SVR and Lasso having better results than MLR. The lower value of MAE, MSE, and RMSE implies higher accuracy of a regression model. However, a higher value of R^2 and the explained variance score, closer to 1 is considered desirable. Figures 8 and 9 indicate that all the models are better performing than lasso and SVR while RF is the best.

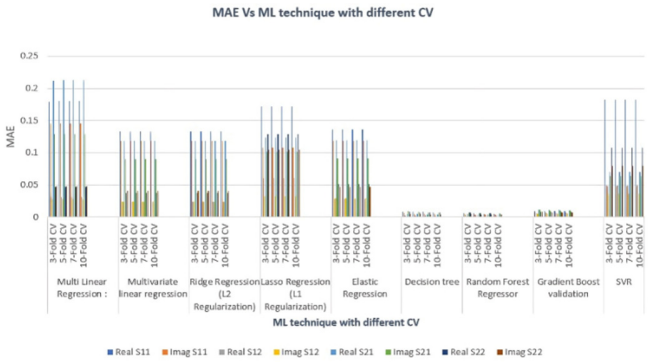

Fig. 5. MAE graph.

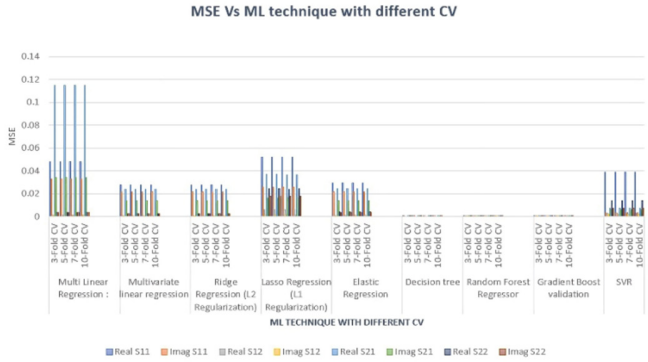

Fig. 6. MSE graph.

Examining the graphical results, it can be noted that RF with 10-fold CV shows the best value at various operating conditions with the least error and highest accuracy for error matrices with average MAE, MSE, RMSE, R^2, EVS as 0.004125, 4.6375×10^{-5}, 0.006475, 0.9977, 0.9977 respectively. Table III depicts the RF algorithm model at all K-folds for all the evaluation matrices, as due to space constraints it was not possible to show the numerical evaluation value for each model. Figure 10 illustrates the extended results with simulation curves at randomly selected bias conditions, further demonstrating the model's effectiveness.

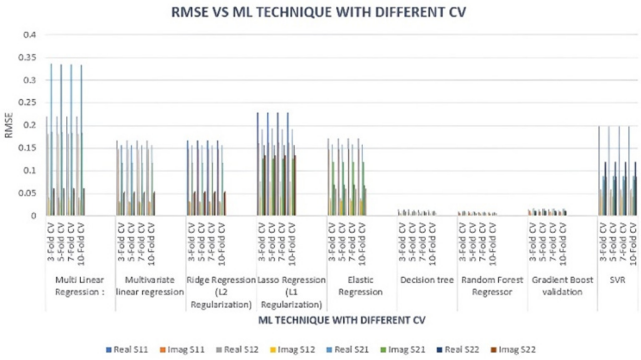

Fig. 7. RMSE graph.

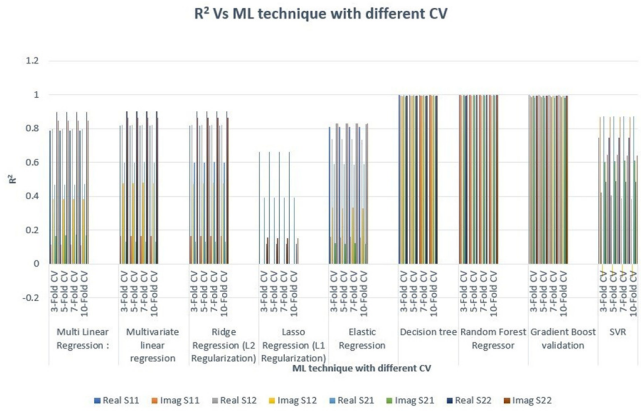

Fig. 8. R^2 graph.

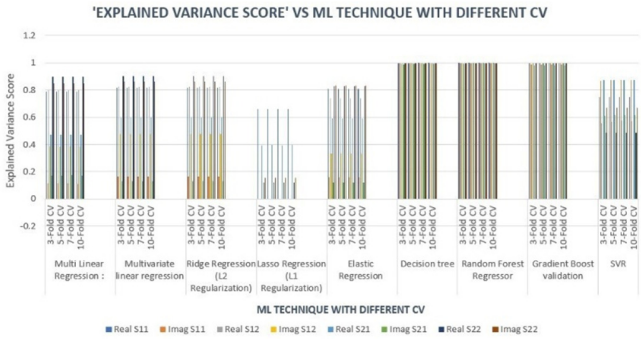

Fig. 9. Explained variance score graph.

TABLE III. OUTCOME OF THE RANDOM FOREST MODEL

	MAE:			
Dependent Variable	**K-Fold (K=3)**	**K-Fold (K=5)**	**K-Fold (K=7)**	**K-Fold (K=10)**
Real(S11)	0.0064	0.0057	0.0054	0.0053
Imag(S11)	0.0051	0.0045	0.0045	0.0043
Real(S12)	0.0033	0.0031	0.003	0.0029
Imag(S12)	0.0015	0.0013	0.0012	0.0012

Real(S21)	0.0052	0.0045	0.0043	0.0041
Imag(S21)	0.0072	0.0062	0.0061	0.0058
Real(S22)	0.0073	0.0062	0.0059	0.0056
Imag(S22)	0.0049	0.0042	0.004	0.0038
MSE:				
Dependent Variable	**K-Fold (K=3)**	**K-Fold (K=5)**	**K-Fold (K=7)**	**K-Fold (K=10)**
Real(S11)	0.00012	0.000092	0.000081	0.000078
Imag(S11)	0.000062	0.000046	0.000047	0.00004
Real(S12)	0.000024	0.00002	0.000019	0.000018
Imag(S12)	0.000009	0.000006	0.000006	0.000006
Real(S21)	0.000094	0.000074	0.000066	0.000061
Imag(S21)	0.000128	0.000095	0.000089	0.000078
Real(S22)	0.000108	0.000072	0.000066	0.000058
Imag(S22)	0.000052	0.00004	0.000035	0.000032
RMSE:				
Dependent Variable	**K-Fold (K=3)**	**K-Fold (K=5)**	**K-Fold (K=7)**	**K-Fold (K=10)**
Real(S11)	0.0109	0.0095	0.0089	0.0088
Imag(S11)	0.0079	0.0068	0.0069	0.0063
Real(S12)	0.0049	0.0045	0.0044	0.0043
Imag(S12)	0.0031	0.0027	0.0026	0.0025
Real(S21)	0.0097	0.0086	0.0081	0.0078
Imag(S21)	0.0113	0.0097	0.0094	0.009
Real(S22)	0.0104	0.0084	0.0081	0.0075
Imag(S22)	0.0072	0.0063	0.0059	0.0056
R2 Score:				
Dependent Variable	**K-Fold (K=3)**	**K-Fold (K=5)**	**K-Fold (K=7)**	**K-Fold (K=10)**
Real(S11)	0.9992	0.9994	0.9995	0.9995
Imag(S11)	0.9976	0.9982	0.9982	0.9984
Real(S12)	0.996	0.9966	0.9968	0.997
Imag(S12)	0.9945	0.9958	0.9959	0.9961
Real(S21)	0.9984	0.9988	0.9989	0.999
Imag(S21)	0.9921	0.9941	0.9945	0.9952
Real(S22)	0.9961	0.9974	0.9976	0.9979
Imag(S22)	0.9976	0.9981	0.9983	0.9985
Explained Variance:				
Dependent Variable	**K-Fold (K=3)**	**K-Fold (K=5)**	**K-Fold (K=7)**	**K-Fold (K=10)**
Real(S11)	0.9992	0.9994	0.9995	0.9995
Imag(S11)	0.9976	0.9982	0.9982	0.9984
Real(S12)	0.996	0.9966	0.9968	0.997
Imag(S12)	0.9945	0.9958	0.9959	0.9961
Real(S21)	0.9984	0.9988	0.9989	0.999
Imag(S21)	0.9921	0.9941	0.9945	0.9952
Real(S22)	0.9961	0.9974	0.9976	0.9979
Imag(S22)	0.9976	0.9981	0.9983	0.9985

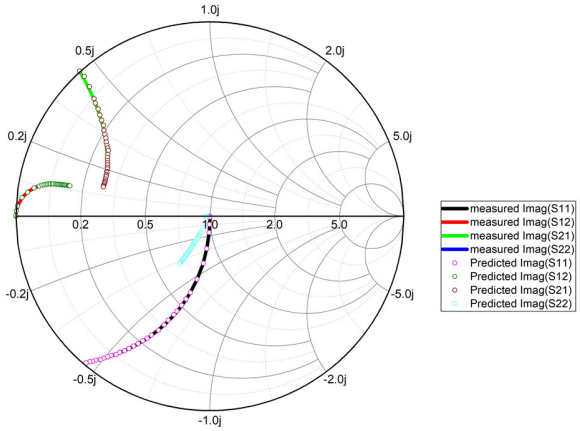

Fig. 10. Measured (line) and predicted (symbols) S-parameters at Vgs=1 V and Vds=15 V for 100 um gate width using RF with 10-fold cross validation.

V. CONCLUSION

In this paper, MLR, MLVR, L2, L1, ENR, DT, RF, GBR, and SVR ML algorithms, were employed to develop GaN HEMT modelling frameworks using different K-fold cross-validations (3, 5, 7, 10). Subsequently, model parameters were tuned to optimize performance. Model generalization was assessed using MSE, MAE, R2, RMSE, and EVS metrics. It was observed that RF with 10-fold **CV** provided the most accurate prediction of the small-signal behavior of GaN HEMT devices, showing the best value at various operating conditions with the least error and highest accuracy for error matrices with average MAE, MSE, RMSE, R2, EVS as 0.004125, 4.6375×10^{-5}, 0.006475, 0.9977, 0.9977, respectively. DT and GBR also yielded promising results. Conversely, SVR and lasso, ENR were deemed unsuitable for GaN HEMT device modeling. There is no universally optimal modeling approach, but rather a range of situations where one approach may be more suitable than another, depending on the existing specific limitations and demands. Looking ahead, further extensive research is required to explore ensemble learning [40], different modeling based on noise, temperature effect and optimization algorithms [41-42].

ACKNOWLEDGMENT

The work is funded by the All-India Council for Technical Education (AICTE) under the AICTE Doctoral Fellowship PhD scheme. The authors would also like to thank DTU for providing software facilities.

REFERENCES

[1] R. Chu and K. Shinohara, *III-Nitride Electronic Devices*. Cambridge, MA, USA: Academic Press, 2019.

[2] J. Xu and D. Chen, "A Performance Comparison of GaN E-HEMTs Versus SiC MOSFETs in Power Switching Applications," *Bodo´s Power Systems*, pp. 36–39, Jun. 2017.

[3] M. Haziq, S. Falina, A. A. Manaf, H. Kawarada, and M. Syamsul, "Challenges and Opportunities for High-Power and High-Frequency AlGaN/GaN High-Electron-Mobility Transistor (HEMT) Applications: A Review," *Micromachines*, vol. 13, no. 12, Dec. 2022, Art. no. 2133, https://doi.org/10.3390/mi13122133.

[4] M. Asif Khan, A. Bhattarai, J. N. Kuznia, and D. T. Olson, "High electron mobility transistor based on a GaN-AlxGa1−xN heterojunction," *Applied Physics Letters*, vol. 63, no. 9, pp. 1214–1215, Aug. 1993, https://doi.org/10.1063/1.109775.

[5] T. Fernandez *et al.*, "Modelling reliability in GaN HEMT devices," in *8th Conference on Simulation, Modelling and Optimization*, Stevens Point, WI, USA, Sep. 2008, pp. 315–318.

[6] G. Crupi *et al.*, "Accurate Multibias Equivalent-Circuit Extraction for GaN HEMTs," *IEEE Transactions on Microwave Theory and Techniques*, vol. 54, no. 10, pp. 3616–3622, Oct. 2006, https://doi.org/10.1109/TMTT.2006.882403.

[7] A. Jarndal and G. Kompa, "A new small-signal modeling approach applied to GaN devices," *IEEE Transactions on Microwave Theory and Techniques*, vol. 53, no. 11, pp. 3440–3448, Nov. 2005, https://doi.org/10.1109/TMTT.2005.857332.

[8] R. G. Brady, C. H. Oxley, and T. J. Brazil, "An Improved Small-Signal Parameter-Extraction Algorithm for GaN HEMT Devices," *IEEE Transactions on Microwave Theory and Techniques*, vol. 56, no. 7, pp. 1535–1544, Jul. 2008, https://doi.org/10.1109/TMTT.2008.925212.

[9] A. Zarate-de Landa, J. E. Zuniga-Juarez, J. R. Loo-Yau, J. A. Reynoso-Hernandez, M. del C. Maya-Sanchez, and J. L. del Valle-Padilla, "Advances in Linear Modeling of Microwave Transistors," *IEEE*

Microwave Magazine, vol. 10, no. 2, pp. 100, 102–111, 146, Apr. 2009, https://doi.org/10.1109/MMM.2008.931675.

[10] G. Crupi, D. M. M.-P. Schreurs, and A. Caddemi, "On the small signal modeling of advanced microwave FETs: A comparative study," *International Journal of RF and Microwave Computer-Aided Engineering*, vol. 18, no. 5, pp. 417–425, 2008, https://doi.org/10.1002/mmce.20300.

[11] G. Crupi, A. Caddemi, D. M. M.-P. Schreurs, and G. Dambrine, "The large world of FET small-signal equivalent circuits," *International Journal of RF and Microwave Computer-Aided Engineering*, vol. 26, no. 9, pp. 749–762, 2016, https://doi.org/10.1002/mmce.21028.

[12] G. Crupi *et al.*, "High-Frequency Extraction of the Extrinsic Capacitances for GaN HEMT Technology," *IEEE Microwave and Wireless Components Letters*, vol. 21, no. 8, pp. 445–447, Aug. 2011, https://doi.org/10.1109/LMWC.2011.2160525.

[13] A. R. Alt, D. Marti, and C. R. Bolognesi, "Transistor Modeling: Robust Small-Signal Equivalent Circuit Extraction in Various HEMT Technologies," *IEEE Microwave Magazine*, vol. 14, no. 4, pp. 83–101, Jun. 2013, https://doi.org/10.1109/MMM.2013.2248593.

[14] V. Dordevic, Z. Marinkovic, V. Markovic, and O. Pronic-Rancic, "Development and validation of ANN approach for extraction of MESFET/HEMT noise model parameters," *Electrical Engineering*, vol. 100, no. 2, pp. 645–651, Jun. 2018, https://doi.org/10.1007/s00202-017-0526-2.

[15] A. Abubakr, A. Hassan, A. Ragab, S. Yacout, Y. Savaria, and M. Sawan, "High-Temperature Modeling of the I-V Characteristics of GaN150 HEMT Using Machine Learning Techniques," in *IEEE International Symposium on Circuits and Systems*, Florence, Italy, Dec. 2018, pp. 1–5, https://doi.org/10.1109/ISCAS.2018.8351508.

[16] Z. Marinkovic *et al.*, "Neural approach for temperature-dependent modeling of GaN HEMTs," *International Journal of Numerical Modelling: Electronic Networks, Devices and Fields*, vol. 28, no. 4, pp. 359–370, 2015, https://doi.org/10.1002/jnm.2011.

[17] A. Jarndal, S. Hamdan, and M. Bettayeb, "On Neural Networks Modeling Based on GA, PSO and GW Optimization Techniques," in *8th International Conference on Modeling Simulation and Applied Optimization*, Manama, Bahrain, Apr. 2019, pp. 1–5, https://doi.org/10.1109/ICMSAO.2019.8880450.

[18] S. Husain, B. Kadirbay, A. Jarndal, and M. Hashmi, "Comprehensive Investigation of ANN Algorithms Implemented in MATLAB, Python, and R for Small-Signal Behavioral Modeling of GaN HEMTs," *IEEE Journal of the Electron Devices Society*, vol. 11, pp. 559–572, 2023, https://doi.org/10.1109/JEDS.2023.3324084.

[19] Z. Marinkovic, G. Crupi, A. Caddemi, V. Markovic, and D. M. M.-P. Schreurs, "A review on the artificial neural network applications for small-signal modeling of microwave FETs," *International Journal of Numerical Modelling: Electronic Networks, Devices and Fields*, vol. 33, no. 3, 2020, Art. no. e2668, https://doi.org/10.1002/jnm.2668.

[20] M. Geng *et al.*, "Modified small-signal behavioral model for GaN HEMTs based on support vector regression," *International Journal of RF and Microwave Computer-Aided Engineering*, vol. 31, no. 9, 2021, Art. no. e22774, https://doi.org/10.1002/mmce.22774.

[21] M. Geng, J. Cai, C. Yu, J. Su, and J. Liu, "Piecewise Small Signal Behavioral Model for GaN HEMTs based on Support Vector Regression," in *IEEE MTT-S International Conference on Numerical Electromagnetic and Multiphysics Modeling and Optimization (NEMO)*, Hangzhou, China, Dec. 2020, pp. 1–3, https://doi.org/10.1109/NEMO49486.2020.9343555.

[22] A. Jarndal, S. Husain, and M. Hashmi, "Genetic algorithm initialized artificial neural network based temperature dependent small-signal modeling technique for GaN high electron mobility transistors," *International Journal of RF and Microwave Computer-Aided Engineering*, vol. 31, no. 3, 2021, Art. no. e22542, https://doi.org/10.1002/mmce.22542.

[23] A. Jarndal, S. Husain, and M. Hashmi, "On temperature-dependent small-signal modelling of GaN HEMTs using artificial neural networks and support vector regression," *IET Microwaves, Antennas & Propagation*, vol. 15, no. 8, pp. 937–953, 2021, https://doi.org/10.1049/mia2.12112.

[24] A. Jarndal, S. Husain, M. Hashmi, and F. M. Ghannouchi, "Large-Signal Modeling of GaN HEMTs Using Hybrid GA-ANN, PSO-SVR, and GPR-Based Approaches," *IEEE Journal of the Electron Devices Society*, vol. 9, pp. 195–208, 2021, https://doi.org/10.1109/JEDS.2020.3035628.

[25] A. S. Hussein and A. H. Jarndal, "On hybrid model parameter extraction of GaN HEMTs based on GA, PSO, and ABC optimization," in *International Conference on Electrical and Computing Technologies and Applications*, Ras Al Khaimah, United Arab Emirates, Nov. 2017, pp. 1–5, https://doi.org/10.1109/ICECTA.2017.8252069.

[26] A. Jarndal, "On neural networks based electrothermal modeling of GaN devices," *IEEE Access*, vol. 7, pp. 94205–94214, Jul. 2019, https://doi.org/10.1109/ACCESS.2019.2928392.

[27] A. Khusro, M. S. Hashmi, and A. Q. Ansari, "Exploring Support Vector Regression for Modeling of GaN HEMT," in *IEEE MTT-S International Microwave and RF Conference*, Kolkata, India, Nov. 2018, pp. 1–3, https://doi.org/10.1109/IMaRC.2018.8877341.

[28] A. Khusro, M. S. Hashmi, A. Q. Ansari, and M. Auyenur, "A new and Reliable Decision Tree Based Small-Signal Behavioral Modeling of GaN HEMT," in *62nd International Midwest Symposium on Circuits and Systems*, Dallas, TX, USA, Aug. 2019, pp. 303–306, https://doi.org/10.1109/MWSCAS.2019.8885334.

[29] A. Khusro, S. Husain, M. S. Hashmi, M. Auyuneur, and A. Q. Ansari, "A Reliable and Fast ANN Based Behavioral Modeling Approach for GaN HEMT," in *16th International Conference on Synthesis, Modeling, Analysis and Simulation Methods and Applications to Circuit Design*, Lausanne, Switzerland, Jul. 2019, pp. 277–280, https://doi.org/10.1109/SMACD.2019.8795247.

[30] A. Khusro, M. S. Hashmi, and A. Q. Ansari, "Enabling the development of accurate intrinsic parameter extraction model for GaN HEMT using support vector regression (SVR)," *IET Microwaves, Antennas & Propagation*, vol. 13, no. 9, pp. 1457–1466, 2019, https://doi.org/10.1049/iet-map.2018.6039.

[31] A. Khusro, S. Husain, M. S. Hashmi, and A. Q. Ansari, "Small signal behavioral modeling technique of GaN high electron mobility transistor using artificial neural network: An accurate, fast, and reliable approach," *International Journal of RF and Microwave Computer-Aided Engineering*, vol. 30, no. 4, 2020, Art. no. e22112, https://doi.org/10.1002/mmce.22112.

[32] A. Khusro, S. Husain, M. S. Hashmi, A. Q. Ansari, and S. Arzykulov, "A Generic and Efficient Globalized Kernel Mapping-Based Small-Signal Behavioral Modeling for GaN HEMT," *IEEE Access*, vol. 8, pp. 195046–195061, 2020, https://doi.org/10.1109/ACCESS.2020.3033788.

[33] S. Husain, A. Khusro, M. Hashmi, G. Nauryzbayev, and M. A. Chaudhary, "Demonstration of CAD Deployability for GPR Based Small-Signal Modelling of GaN HEMT," in *IEEE International Symposium on Circuits and Systems*, Daegu, Korea, Dec. 2021, pp. 1–5, https://doi.org/10.1109/ISCAS51556.2021.9401088.

[34] S. Husain, M. Hashmi, A. Jarndal, M. Chaudhary, and G. Nauryzbayev, "Comparative Analysis of ANN Architectures for the Development of GaN HEMT Small-Signal Model," in *IEEE MTT-S International Microwave and RF Conference*, Kanpur, India, Dec. 2021, pp. 1–4, https://doi.org/10.1109/IMaRC49196.2021.9714637.

[35] A. Mishra *et al.*, "Multilayer perceptron–random forest based hybrid machine learning–neural network model for GaN high electron mobility transistor's parameter estimations," *International Journal of RF and Microwave Computer-Aided Engineering*, vol. 32, no. 7, 2022, Art. no. e23191, https://doi.org/10.1002/mmce.23191.

[36] S. Husain, M. Hashmi, and F. M. Ghannouchi, "Comprehensive Investigation and Comparative Analysis of Machine Learning-Based Small-Signal Modelling Techniques for GaN HEMTs," *IEEE Journal of the Electron Devices Society*, vol. 10, pp. 1015–1032, 2022, https://doi.org/10.1109/JEDS.2022.3224433.

[37] S. Husain, A. Jarndal, M. Hashmi, and F. M. Ghannouchi, "Accurate, Efficient and Reliable Small-Signal Modeling Approaches for GaN HEMTs," *IEEE Access*, vol. 11, pp. 106833–106846, 2023, https://doi.org/10.1109/ACCESS.2023.3317530.

[38] M. Pal and P. Bharati, *Applications of Regression Techniques*. Berlin, Germany: Springer, 2019.

[39] D. Chicco, M. J. Warrens, and G. Jurman, "The coefficient of determination R-squared is more informative than SMAPE, MAE, MAPE, MSE and RMSE in regression analysis evaluation," *PeerJ Computer Science*, vol. 7, Jul. 2021, Art. no. e623, https://doi.org/10.7717/peerj-cs.623.

[40] A. S. Alkarim, A. S. A.-M. Al-Ghamdi, and M. Ragab, "Ensemble Learning-based Algorithms for Traffic Flow Prediction in Smart Traffic Systems," *Engineering, Technology & Applied Science Research*, vol. 14, no. 2, pp. 13090–13094, Apr. 2024, https://doi.org/10.48084/etasr.6767.

[41] F. Bagheri, N. Ghafarnia, and F. Bahrami, "Electrocardiogram (ECG) Signal Modeling and Noise Reduction Using Hopfield Neural Networks," *Engineering, Technology & Applied Science Research*, vol. 3, no. 1, pp. 345–348, Feb. 2013, https://doi.org/10.48084/etasr.243.

[42] N. K. Al-Shammari *et al.*, "Cardiac Stroke Prediction Framework using Hybrid Optimization Algorithm under DNN," *Engineering, Technology & Applied Science Research*, vol. 11, no. 4, pp. 7436–7441, Aug. 2021, https://doi.org/10.48084/etasr.4277.